Changes in the high latitude Southern Hemisphere through the Eocene-Oligocene Transition: a model-data comparison (Supplementary Material)

Alan T. Kennedy-Asser[1,2], Daniel J. Lunt[1,2], Paul J. Valdes[1,2], Jean-Baptiste Ladant[3], Joost Frieling[4], Vittoria Lauretano[2,5]

[1] BRIDGE, School of Geographical Sciences, University of Bristol, Bristol, UK
[2] Cabot Institute for the Environment, University of Bristol, Bristol, UK
[3] Department of Earth and Environmental Sciences, University of Michigan, Ann Arbor, USA
[4] Marine Palynology and Paleoceanography, Laboratory of Palaeobotany and Palynology, Department of Earth Sciences, Faculty of Geosciences, Utrecht University, Princetonlaan 8a, 3584CB Utrecht, the Netherlands
[5] Organic Geochemistry Unit, School of Chemistry, University of Bristol, Bristol, UK

Correspondence to: Alan T. Kennedy-Asser (alan.kennedy@bristol.ac.uk)

Abstract. Global and regional climate changed dramatically with the expansion of the Antarctic Ice sheet at the Eocene-Oligocene Transition (EOT). These large-scale changes are generally linked to declining atmospheric pCO_2 levels and/or changes in Southern Ocean gateways such as the Drake Passage around this time. To better understand the Southern Hemisphere regional climatic changes and the impact of glaciation on the Earth's oceans and atmosphere at the EOT, we compiled a database of sea and land surface temperature reconstructions from a range of proxy records and compared this with a series of fully-coupled climate model simulations. Regional patterns in the proxy records of temperature show that cooling across the EOT was less at high latitudes and greater at mid-latitudes. Climate model simulations have some issues in capturing the zonal mean latitudinal temperature profiles shown by the proxy data, but certain simulations do show moderate-good performance at recreating the temperature patterns shown in the data. When taking into account the absolute temperature before and after the EOT, as well as the change in temperature across it, simulations with a closed Drake Passage before and after the EOT or with an opening of the Drake Passage across the EOT perform poorly, whereas simulations with a drop in atmospheric pCO_2 in combination with ice growth generally perform better. This provides further support to previous research that changes in atmospheric pCO_2 are more likely to have been the driver of the EOT climatic changes, as opposed to opening of the Drake Passage.

1 Introduction

This supplementary information gives an overview of the three temperature datasets compiled for the late Eocene absolute temperatures, early Oligocene absolute temperatures and relative change in temperatures across the EOT (Section 2). Additionally, it provides some further information on the model simulation pairs used to simulate change across the EOT

(Section 3) as well as examples of how the error between model and proxy data is calculated for the RMSE metrics (Section 4). Finally, it includes full references for all of the data used in the compilations.

2 Datasets

A full digital version of each dataset is available from the Open Science Framework (Kennedy-Asser, 2019).

Table S1: Compilation of temperature proxy records for the late Eocene.

Site	Palaeo-Lat.	Palaeo-Long.	Mean annual temp. (MAT; °C)	Max. MAT (°C)	Min. MAT (°C)	Proxy description	Age max. (Ma)	Age min. (Ma)	Source
Maud Rise	-65.3	1.6	12.3	13.3	11.3	Clumped isotopes	35.3	34.2	Value from Petersen & Schrag, 2015 (Table 2)
Prydz Bay	-66.2	73.0		12.0		Veg. NLR	39.0	34.0	Maximum value given in Trusswell & Macphail, 2009 (p. 100)
Prydz Bay	-66.2	73.0	10.3	13.9	6.7	S-index	35.8	33.7	Value from Passchier et al., 2016 (supp. info.), error from main text (p. 2)
Prydz Bay	-66.2	73.0		10.0		Dinocysts	35.4	33.6	Value from Houben et al., 2013, (Figure 3) and Zonnefeld et al., 2013 (Figure 208)
Kerguelen Plateau	-58.6	79.8	14.3	15.3	13.3	Mg/Ca	35.3	34.2	Offset from Maud Rise by 2°C, value in Bohaty et al., 2012, (Section 4.1)
Wilkes Land U1356	-61.1	130.3				No data			
Wilkes Land U1360	-66.3	136.8				No data			
S. Australia	-54.4	144.8	17.0	20.0	14.0	Veg. NLR	35.0	34.0	Korasidis et al. 2019 temperature estimate for T0 coal seam (mean between max. and min. range). Age is approximate based on Fig. 6.
S. Australia (region)	-54.4	144.8	16.0	20.6	11.3	Veg. Coexist.	36.6	34.0	Max. and min. values quoted in Pound & Salzmann, 2017 (p.4), location assumed the same as Korasidis et al.; mean taken between the max. and min. may be unrealistic
East Tasman Plateau	-60.7	152.9	22.4	24.9	19.9	TEX_{86}	37.0	33.7	Values from Houben et al. 2019 supplementary information (Molecular Paleothermometry tab). Mean is average of $TEX_{86}H$ calibration for values with BIT index <0.4 and depth 360-367.5 mbsf. Calibration error is taken as 2.5 from main text (p. 2218).

East Tasman Plateau	-60.7	152.9		10.0		Dinocysts	35.5	33.7	Value from Houben et al., 2013, (Figure 3) and Zonnefeld et al., 2013 (Figure 208)
Ross Sea	-76.7	155.9		13.0		Veg. NLR	41.0	34.0	Value from Francis et al., 2009 (p.333), location assumed the same as CRP-3 and age assumed 41-34 Ma (Bartonian/Priabonian)
Ross Sea	-76.7	155.9	8.7	12.3	5.1	S-index	36.2	34.2	Value from Passchier et al., 2013 (supp. info.; MAT sheet), error from main text (p. 1403)
New Zealand	-59.4	176.6	25.9	27.1	24.7	TEX_{86}	35.4	33.6	Value and error from Liu et al., 2009 (supp. info.), error of 2 stan. dev.
New Zealand	-59.4	176.6	25.6	27.6	23.6	$U^{K'}_{37}$	35.4	33.6	Value and error from Liu et al., 2009 (supp. info.), error of 2 stan. dev.
King George Isl.	-63.8	-62.6	10.0	15.0	5.0	Veg. NLR	41.0	34.0	Max. value from Birkenmajer & Zastawniak, 1989, main text (p. 238), date from main text (p. 234, discussion of loc. 7); Min. value from Francis et al. 2009 (p.330-331); mean taken between the max. and min. may be unrealistic
Seymour Isl.	-66.3	-58.4	12.8	16.0	9.2	Clumped isotopes	37.5	34.0	Value from Douglas et al., 2014 (supp. info., Table S3: mean of 34, 37.4 and 37.5 Ma values for both *Cucullaea* and *Eurhomalea*), error from maximum range of these values with their external error
Seymour Isl.	-66.3	-58.4	11.6	17.0	9.0	TEX_{86}	37.5	34.0	Value from Douglas et al., 2014 (supp. info., Table S4: mean of 34, 37.4 and 37.4 Ma TEX86L and TEX86' values), error from main text (p.4)
Seymour Isl.	-66.3	-58.4	16.5	22.3	10.7	MBT-CBT	37.5	34.0	Values from Douglas et al., 2014, (supp. info., Table S4: mean of 34, 37.4 and 37.5 Ma values). Two calibrations give very different values, taken here as a max. and min. range; mean (of max. and min.) may therefore be unrealistic
Weddell Sea	-64.0	-40.7		10.0		Dinocysts	36.6	33.6	Value from Houben et al., 2013, (Figure 3) and Zonnefeld et al., 2013 (Figure 208)
Falklands Plateau	-53.1	-38.6	18.4	22.0	14.8	TEX_{86}	37.1	33.3	Value and error from Liu et al., 2009 (supp. info.), error of 2 stan. dev.
Falklands Plateau	-53.1	-38.6	18.1	20.6	15.6	TEX_{86}	37.0	34.0	Values from Houben et al. 2019 supplementary information (Molecular Paleothermometry tab). Mean is average of $TEX_{86}H$ calibration for values with BIT index <0.4 and depth 138-180 mbsf

									(depth-ages taken from Liu et al. 2009 supp. info.). Calibration error is taken as 2.5 from main text (p. 2218).
Falklands Plateau	-53.1	-38.6	19.5	23.7	15.3	$U^{K'}_{37}$	37.1	33.3	Value and error from Liu et al., 2009 (supp. info.), error of 2 stan. dev.
S.W. Atlantic (region)	-60.0	-60.0	15.9	18.4	13.4	Veg. Coexist.	37.0	34.0	Max. and min. values quoted in Pound & Salzmann, 2017 (p.5), location is very large/unspecified, mean taken between the max. and min. may be unrealistic

40

Table S2: Compilation of temperature proxy records for the early Oligocene.

Site	Palaeo-Lat.	Palaeo-Long.	Mean annual temp. (MAT; °C)	Max. MAT (°C)	Min. MAT (°C)	Proxy description	Age max. (Ma)	Age min. (Ma)	Source
Maud Rise	-65.3	1.6	11.9	12.2	11.6	Clumped isotopes	33.0	31.9	Value from Petersen & Schrag, 2015 (Table 2)
Prydz Bay	-66.2	73.0	8.0	11.6	4.4	S-index	33.7	32.9	Value from Passchier et al., 2016 (supp. info.), error from main text (p. 2)
Prydz Bay	-66.2	73.0		10.0		Dinocysts	33.6	33.3	Value from Houben et al., 2013, (Figure 3) and Zonnefeld et al., 2013 (Figure 208)
Kerguelen Plateau	-58.6	79.8	11.7	13.5	9.9	Mg/Ca	34.0	33.2	Value from Bohaty et al., section 4.2, taken away from inferred late Eocene temp.; max. and min. allowing for error in absolute values (from Petersen & Schrag 2015) and change (Bohaty et al., 2012)
Wilkes Land U1356	-61.1	130.3	8.9	12.5	5.3	S-index	33.6	30.0	Value from Passchier et al. 2013 supp. info. (MAT sheet), error from main text (p. 1403)
Wilkes Land U1356	-61.1	130.3		10.0		Dinocysts	33.5	30.5	Value from Houben et al. 2013 figure 3 and Zonnefeld et al. 2013 figure 208
Wilkes Land U1356	-61.1	130.3	17.5	21.5	13.5	TEX_{86}	33.1	32.9	Value from Hartman et al. 2018 (reading first three points in record shown in Figure 3), with 4°C calibration error based on main text (p. 1285)
Wilkes Land U1360	-66.3	136.8		10.0		Dinocysts	33.6	32.4	Value from Houben et al. 2013 figure 3 and Zonnefeld et al. 2013 figure 208
S. Australia	-54.4	144.8	12.0	14.0	10.0	Veg. NLR	30.0	29.0	Korasidis et al. 2019 temperature estimate for M2A coal seam (mean

									between max. and min. range). Age is approximate based on Fig. 6.
S. Australia (region)	-54.4	144.8	16.0	20.6	11.3	Veg. Coexist.	33.0	30.0	Max. and min. values quoted in Pound & Salzmann, 2017 (p.4), location assumed the same as Korasidis et al. data; mean taken between the max. and min. may be unrealistic
East Tasman Plateau	-60.7	152.9	22.4	24.9	19.9	TEX_{86}	33.7	30.0	Values from Houben et al. 2019 supplementary information (Molecular Paleothermometry tab). Mean is average of $TEX_{86}H$ calibration for values with BIT index <0.4 and depth 358-360
Ross Sea	-76.7	155.9		10.0		Dinocysts	32.5	31.0	Value from Houben et al. 2013 figure 3 and Zonnefeld et al. 2013 figure 208
Ross Sea	-76.7	155.9	7.8	11.4	4.2	S-index	33.6	33.0	Value from Passchier et al., 2013 (supp. info.; MAT sheet), error from main text (p. 1403)
Ross Sea	-76.7	155.9	-2.0	8.0	-12.0	Vegetation NLR	32.0	31.0	Max. value from Passchier et al. 2013 supp. info. (vegetation sheet), based on their interpretation of similar modern ecosystem. Minimum value based on interpretations of Francis & Hill 1996. Approx. age from Prebble et al. 2006
New Zealand	-59.4	176.6	23.8	24.8	22.8	TEX_{86}	33.6	33.4	Value and error from Liu et al., 2009 (supp. info.), error of 2 stan. dev.
New Zealand	-59.4	176.6	22.4	23.8	21.0	$U^{K'}_{37}$	33.6	33.4	Value and error from Liu et al., 2009 (supp. info.), error of 2 stan. dev.
King George Isl.	-63.8	-62.6				No data			
Seymour Isl.	-66.3	-58.4				No data			
Weddell Sea	-64.0	-40.7		10.0		Dinocysts	33.6	33.2	Value from Houben et al., 2013, (Figure 3) and Zonnefeld et al., 2013 (Figure 208)
Falklands Plateau	-53.1	-38.6	11.2	14.4	8.0	TEX_{86}	33.7	33.1	Value and error from Liu et al., 2009 (supp. info.), error of 2 stan. dev.
Falklands Plateau	-53.1	-38.6	16.0	18.5	13.5	TEX_{86}	33.7	32.0	Values from Houben et al. 2019 supplementary information (Molecular Paleothermometry tab). Mean is average of $TEX_{86}H$ calibration for values with BIT index <0.4 and depth 20-130 mbsf (depth-ages taken from Liu et al. 2009 supp. info.). Calibration error is taken as 2.5 from main text (p. 2218).

Falklands Plateau	-53.1	-38.6	11.1	13.7	8.5	$U^{K'}_{37}$	33.7	33.1	Value and error from Liu et al., 2009 (supp. info.), error of 2 stan. dev.
S.W. Atlantic (region)	-60.0	-60.0	17.6	23.4	11.7	Veg. Coexist.	31.1	30.9	Max. and min. values quoted in Pound & Salzmann, 2017 (p.5), location is very large/unspecified, mean taken between the max. and min. may be unrealistic

45

Table S3: Compilation of temperature proxy records across the Eocene-Oligocene Transition.

Site	Palaeo-Lat.	Palaeo-Long.	Mean temp. change (°C)	Max. temp. change (°C)	Min. temp. change (°C)	Proxy description	Source
Maud Rise	-65.3	1.6			0.0	Nannofossils	General cooling suggested from Villa et al., 2013 (Figures 5 and 6)
Maud Rise	-65.3	1.6			0.0	Mg/Ca	General cooling suggested from Bohaty et al., 2012 (Figure 4b)
Maud Rise	-65.3	1.6	-0.4	-1.5	0.7	Clumped isotopes	Value from Petersen & Schrag, 2015 (Table 2)
Prydz Bay	-66.2	73.0			0.0	Dinocysts	*S. antarctica* increase shown in Houben et al., 2013 (Figure 3 and in supplementary dataset)
Prydz Bay	-66.2	73.0	-2.3	-5.1	0.5	S-index	Mean from difference in Passchier et al., 2016 (supp. info.); range taken from difference between max. and min. of each period based on 2 stan. dev.
Kerguelen Plateau	-58.6	79.8	-2.6	-3.4	-1.8	Mg/Ca	Value from Bohaty et al. 2012, section 4.2
Kerguelen Plateau	-58.6	79.8			0.0	Mg/Ca	General trend from Villa et al. 2013, Figure 2, 3 + 4
Wilkes Land U1356	-61.1	130.3				No data	
Wilkes Land U1360	-66.3	136.8				No data	
S. Australia	-54.4	144.8	-5.0	-10.0	0.0	Veg. NLR	Korasidis et al. 2019, Fig. 6 shows cooling, but with a relatively large gap in time between sections. Uncertainty range from difference in max. and min. values around each mean
S. Australia (region)	-54.4	144.8				Veg. Coexist.	Max. and min. values quoted in Pound & Salzmann 2017 (p.4) suggest a dip in MATR before the EOT, rising again to same values after; location assumed the same as Korasidis et al. data; mean taken between the max. and min. may be unrealistic

East Tasman Plateau	-60.7	152.9	0.0	-3.0	3.0	TEX_{86}	Values from Houben et al. 2019 supplementary information (Molecular Paleothermometry tab), TEX86H calibration. Uncertainty range from difference in max. and min. based on 2 SD around each mean. Houben et al. 2019 Fig. 3 shows record is very noisy.
Ross Sea	-76.7	155.9	-1.0	-5.9	4.0	S-index	Value from difference in Passchier et al. 2013 supp. info. (MAT sheet), error taken from extremes of each period calculated with 2 SD
Ross Sea	-76.7	155.9			0.0	Vegetation NLR	Vegetation reconstructions from multiple sources suggest cooler conditions in Oligocene, but estimates of by how much vary significantly
New Zealand	-59.4	176.6	-2.1	-2.9	-1.3	TEX_{86}	Value and error from Liu et al., 2009 (supp. info.)
New Zealand	-59.4	176.6	-3.1	-4.4	-1.8	$U^{K'}_{37}$	Value and error from Liu et al., 2009 (supp. info.)
King George Isl.	-63.8	-62.6				No data	
Seymour Isl.	-66.3	-58.4				No data	
Weddell Sea	-64.0	-40.7			0.0	Dinocysts	Increase shown in Houben et al. 2013 Figure 3 and in supplementary dataset
Falklands Plateau	-53.1	-38.6	-7.2	-9.6	-4.8	TEX_{86}	Value and error from Liu et al., 2009 (supp. info.)
Falklands Plateau	-53.1	-38.6	-2.1	-7.0	2.8	TEX_{86}	Values from Houben et al. 2019 supplementary information (Molecular Paleothermometry tab), TEX86H calibration. Uncertainty range from difference in max. and min. based on 2 SD around each mean
Falklands Plateau	-53.1	-38.6	-8.4	-10.9	-5.9	$U^{K'}_{37}$	Value and error from Liu et al., 2009 (supp. info.)
S.W. Atlantic (region)	-60.0	-60.0				Veg. Coexist.	Max. and min. values quoted in Pound & Salzmann, 2017 (p.5) suggest a dip in MATR before the EOT, rising again after to have wider range; location unclear

3 Model simulation pairs

The model simulations used here have been previously described in Kennedy-Asser et al. (2019) and Ladant et al. (2014). Outlined here in Table S4 are the pairs of model simulations that make up each forcing scenario of the change across the EOT, as used in the model evaluation (Section 3.4). The output data from the HadCM3BL simulations can be freely accessed at: https://www.paleo.bristol.ac.uk/ummodel/scripts/papers/.

Table S4: Model simulation pairings used to represent various forcings across the Eocene-Oligocene Transition.

Model	Description (as in Figure 5)	Eocene setup (*simulation name*)	Oligocene setup (*simulation name*)
		AIS growth	
HadCM3BL	3x, closed DP	AIS: none. pCO_2: 840 ppmv. Drake Passage: closed. (*tecqu2*)	AIS: EAIS. pCO_2: 840 ppmv. Drake Passage: closed. (*tecqt3*)
HadCM3BL	3x, open DP	AIS: none. pCO_2: 840 ppmv. Drake Passage: open. (*tecqv1*)	AIS: EAIS. pCO_2: 840 ppmv. Drake Passage: open. (*tecqs1*)
HadCM3BL	2x, closed DP	AIS: none. pCO_2: 560 ppmv. Drake Passage: closed. (*tecqp2*)	AIS: EAIS. pCO_2: 560 ppmv. Drake Passage: closed. (*tecqo2*)
HadCM3BL	2x, open DP	AIS: none. pCO_2: 560 ppmv. Drake Passage: open. (*tecqq1*)	AIS: EAIS. pCO_2: 560 ppmv. Drake Passage: open. (*tecqn1*)
FOAM	2x (small EAIS)	AIS: none. pCO_2: 560 ppmv. Drake Passage: open. (*FOAM.34Ma.WAM.2x.WSO*)	AIS: small EAIS. pCO_2: 560 ppmv. Drake Passage: open. (*FOAM.34Ma.WAM.2x.WSO.ISS1*)
FOAM	2x (EAIS)	AIS: none. pCO_2: 560 ppmv. Drake Passage: open. (*FOAM.34Ma.WAM.2x.WSO*)	AIS: EAIS. pCO_2: 560 ppmv. Drake Passage: open. (*FOAM.34Ma.WAM.2x.WSO.ISS2*)
FOAM	2x (full AIS)	AIS: none. pCO_2: 560 ppmv. Drake Passage: open. (*FOAM.34Ma.WAM.2x.WSO*)	AIS: full AIS. pCO_2: 560 ppmv. Drake Passage: open. (*FOAM.34Ma.WAM.2x.WSO.ISS3*)
		AIS growth + pCO_2 drop	
HadCM3BL	Closed DP (3x-2x)	AIS: none. pCO_2: 840 ppmv. Drake Passage: closed.	AIS: EAIS. pCO_2: 560 ppmv. Drake Passage: closed.

		(*tecqu2*)	(*tecqo2*)
HadCM3BL	Open DP (3x-2x)	AIS: none. pCO_2: 840 ppmv. Drake Passage: open. (*tecqv1*)	AIS: EAIS. pCO_2: 560 ppmv. Drake Passage: open. (*tecqn1*)
FOAM	Small EAIS + 3x-2x	AIS: none. pCO_2: 840 ppmv. Drake Passage: open. (*FOAM.34Ma.WAM.3x.WSO*)	AIS: small EAIS. pCO_2: 560 ppmv. Drake Passage: open. (*FOAM.34Ma.WAM.2x.WSO.ISS1*)
FOAM	EAIS + 3x-2x	AIS: none. pCO_2: 840 ppmv. Drake Passage: open. (*FOAM.34Ma.WAM.3x.WSO*)	AIS: EAIS. pCO_2: 560 ppmv. Drake Passage: open. (*FOAM.34Ma.WAM.2x.WSO.ISS2*)
FOAM	Full AIS + 3x-2x	AIS: none. pCO_2: 840 ppmv. Drake Passage: open. (*FOAM.34Ma.WAM.3x.WSO*)	AIS: full AIS. pCO_2: 560 ppmv. Drake Passage: open. (*FOAM.34Ma.WAM.2x.WSO.ISS3*)
FOAM	Small EAIS + 4x-2x	AIS: none. pCO_2: 1,120 ppmv. Drake Passage: open. (*FOAM.34Ma.WAM.4x.WSO*)	AIS: small EAIS. pCO_2: 560 ppmv. Drake Passage: open. (*FOAM.34Ma.WAM.2x.WSO.ISS1*)
FOAM	EAIS + 4x-2x	AIS: none. pCO_2: 1,120 ppmv. Drake Passage: open. (*FOAM.34Ma.WAM.4x.WSO*)	AIS: EAIS. pCO_2: 560 ppmv. Drake Passage: open. (*FOAM.34Ma.WAM.2x.WSO.ISS2*)
FOAM	Full AIS + 4x-2x	AIS: none. pCO_2: 1,120 ppmv. Drake Passage: open. (*FOAM.34Ma.WAM.4x.WSO*)	AIS: full AIS. pCO_2: 560 ppmv. Drake Passage: open. (*FOAM.34Ma.WAM.2x.WSO.ISS3*)
		AIS growth + DP opening	
HadCM3BL	3x	AIS: none. pCO_2: 840 ppmv. Drake Passage: closed. (*tecqu2*)	AIS: EAIS. pCO_2: 840 ppmv. Drake Passage: open. (*tecqs1*)
HadCM3BL	2x	AIS: none. pCO_2: 560 ppmv. Drake Passage: closed. (*tecqp2*)	AIS: EAIS. pCO_2: 560 ppmv. Drake Passage: open. (*tecqn1*)
		All	
HadCM3BL	3x-2x, opening DP	AIS: none. pCO_2: 840 ppmv. Drake Passage: closed. (*tecqu2*)	AIS: EAIS. pCO_2: 560 ppmv. Drake Passage: open. (*tecqn1*)

4 Error calculation

As discussed in Section 2.4, for the model-data comparison, the error, E, between the modelled temperature, T_m, and proxy reconstructed temperature, T_p, for a given site and time period, i, is taken between the limits of the uncertainty range from both the modelled and the proxy reconstructed temperatures. If there is any overlap between the uncertainty ranges, E is taken as 0. For proxy records that provide an upper limit to the temperature, if the lower limit from the model is less than the proxy upper limit, E is taken as 0; otherwise E is taken as the difference between the model lower limit and the proxy. Examples of how this is calculated are illustrated in Figure S1.

The error can be calculated in this way for the standard RMSE metric ($E_{S,i}$) using the raw values of temperature from the datasets or model simulations, or for the normalised RMSE metric ($E_{N,i}$) if the mean temperature of all proxy data points/sites is removed from the datasets and simulation data.

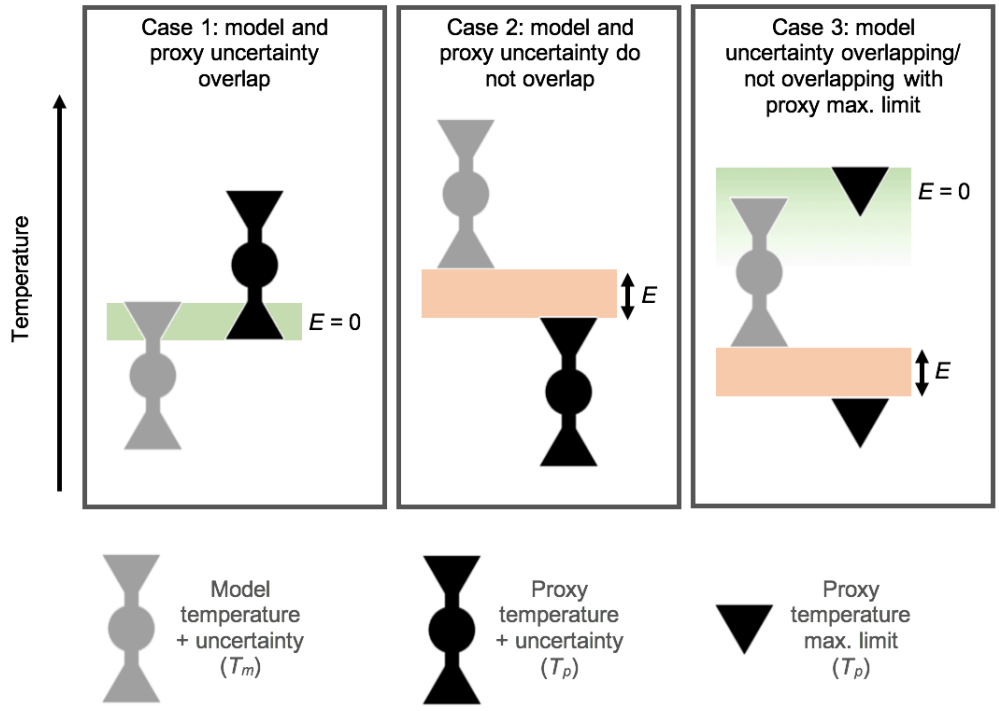

Figure S1: examples of how the error, *E*, is calculated for the standard and normalise RMSE metrics.

References

Birkenmajer, K. & Zastawniak, E.: Late Cretaceous–Early Tertiary floras of King George Island, West Antarctica: their stratigraphic distribution and palaeoclimatic significance, In: Crame, J.A. (Ed.), Origins and Evolution of the Antarctic Biota, Geological Society Special Publication 147, pp. 227–240, 1989.

Bohaty, S.M., Zachos, J.C. & Delaney, M.L.: Foraminiferal Mg/Ca evidence for Southern Ocean cooling across the Eocene-Oligocene transition, *Earth and Planetary Science Letters*, 317-318, pp. 251-261, DOI: 10.1016/j.epsl.2011.11.037, 2012.

Douglas, P.M.J., Affek, H.P., Ivany, L.C., Houben, A.J.P., Sijp, W.P., Sluijs, A., Schouten, S. & Pagani, M.: Pronounced zonal heterogeneity in Eocene southern high-latitude sea surface temperatures, *PNAS*, 111, 18, pp. 6582-6587, DOI: 10.1073/pnas.1321441111, 2014.

Francis, J.S. & Hill, R.S.: Fossil Plants from the Pliocene Sirius Group, Transantarctic Mountains: Evidence for Climate from Growth Rings and Fossil Leaves, *Palaios*, 11, 4, pp. 389-396, 1996.

Francis, J.E., Marenssi, S., Levy, R., Hambrey, M, Thorn, V.T., Mohr, B., Brinkhuis, H., Warnaar, J., Zachos, J.C., Bohaty, S.M., & DeConto, R.M.: From Greenhouse to Icehouse – The Eocene/Oligocene in Antarctica. In: Developments in Earth & Environmental Sciences, 8, F. Florindo and M. Siegert (Editors), DOI 10.1016/S1571-9197(08)00008-6, 2009.

Hartman, J.D., Sangiorgi, F., Salabarnada, A., Peterse, F., Houben, A.J.P., Schouten, S., Brinkhuis, H., Escutia, C. & Bijl, P.K.: Paleoceanography and ice sheet variability offshore Wilkes Land, Antarctica – Part 3: Insights from Oligocene–Miocene TEX_{86}-based sea surface temperature reconstructions, *Climate of the Past*, 14, pp. 1275-1297, DOI: 10.5194/cp-14-1275-2018, 2018.

Houben, A.J.P., Bijl, P.K., Pross, J., Bohaty, S.M., Passchier, S., Stickley, C.E., Röhl, U., Sugisaki, S., Tauxe, L., van de Flierdt, T., Olney, M., Sangiorgi, F., Sluijs, A., Escutia, C., Brinkhuis, H.A. & the Expedition 318 Scientists: Reorganization of Southern Ocean Plankton Ecosystem at the Onset of Antarctic Glaciation, *Science*, 340, pp. 341-344, DOI: 10.1126/science.1223646, 2013.

Houben, A. J. P., Bijl, P. K., Sluijs, A., Schouten, S. & Brinkhuis, H.: Late Eocene Southern Ocean cooling and invigoration of circulation preconditioned Antarctica for full-scale glaciation, *Geochemistry, Geophysics, Geosystems*, 20, pp. 2214–2234. DOI: 10.1029/2019GC008182, 2019.

Kennedy-Asser, A.T., Lunt, D.J., Farnsworth, A. & Valdes, P.J: Assessing mechanisms and uncertainty in modelled climatic change at the Eocene-Oligocene Transition, *Paleoceanography and Paleoclimatology*, 34, pp. 16-34, DOI: 10.1029/2018PA003380, 2019.

Kennedy-Asser, A. T.: EOT_SOcean (accessed 29th August 2019), https://doi.org/10.17605/OSF.IO/BKN26, 2019.

Korasidis, V.A., Wallace, M.W., Wagstaff, B.E. & Hill, R.S.: Terrestrial cooling record through the Eocene-Oligocene transition of Australia, *Global and Planetary Change*, 173, pp. 61-72, DOI: 10.1016/j.gloplacha.2018.12.007, 2019.

Ladant, J.B., Donnadieu, Y., Lefebvre, V. & Dumas, C.: The respective role of atmospheric carbon dioxide and orbital parameters on ice sheet evolution at the Eocene-Oligocene transition, *Paleoceanography*, DOI: 10.1002/2013PA002593, 2014.

Liu, Z., Pagani, M., Zinniker, D., DeConto, R., Huber, M., Brinkhuis, H., Shah, S.R., Leckie, R.M., & Pearson, A.: Global cooling during the Eocene–Oligocene climate transition, *Science*, 323, pp. 1187-1190, DOI: 10.1126/science.1166368, 2009.

Passchier, S., Bohaty, S.M., Jiménez-Espejo, F., Pross, J., Röhl, U., van de Flierdt, T., Escutia, C. & Brinkhuis, H.: Early Eocene to middle Miocene cooling and aridification of East Antarctica, *Geochemistry, Geophysics, Geosystems*, 14, 5, pp. 1399-1410, DOI: 10.1002/ggge.20106, 2013.

Passchier, S., Ciarletta, D.J., Miriagos, T.E., Bijl, P.K. & Bohaty, S.M.: An Antarctic stratigraphic record of stepwise ice growth through the Eocene-Oligocene transition, *GSA Bulletin*, DOI: 10.1130/B31482.1, 2016.

Petersen, S.V. & Schrag, D.P.: Antarctic ice growth before and after the Eocene-Oligocene transition: New estimates from clumped isotope paleothermometry, *Paleoceanography*, 30, pp. 1305-1317, DOI: 10.1002/2014PA002769, 2015.

Pound, M.J. & Salzmann, U.: Heterogeneity in global vegetation and terrestrial climate change during the late Eocene to early Oligocene transition, *Scientific Reports*, 7, p. 43386, DOI: 10.1038/srep43386, 2017.

Prebble, J.G., Raine, J.I., Barrett, P.J. & Hannah, M.J.: Vegetation and climate from two Oligocene glacioeustatic sedimentary cycles (31 and 24 Ma) cored by the Cape Roberts Project, Victoria Land Basin, Antarctica, *Palaeogeography, Palaeoclimatology, Palaeoecology*, 231, pp. 41-57, DOI: 10.1016/j.palaeo.2005.07.025, 2006.

Trusswell, E.M. & Macphail, M.K.: Polar forests on the edge of extinction: what does the fossil spore and pollen evidence from East Antarctica say? *Australian Systematic Botany*, 22, pp. 57-106, DOI: 10.1071/SB08046, 2009.

Villa, G., Fioroni, C., Persico, D., Roberts, A.P. & Florindo, F.: Middle Eocene to Late Oligocene Antarctic glaciation/deglaciation and Southern Ocean productivity, *Paleoceanography*, 29, pp. 223-237, DOI: 10.1002/2013PA002518, 2013.

Zonneveld, K.A.F., Marret, F., Versteegh, G.J.M., Bogus, K., Bonnet, S., Bouimetarhan, I., Crouch, E., de Vernal, A., Elshanawany, R., Edwards, L., Esper, O., Forke, S., Grøsfjeld, K., Henry, M., Holzwarth, U., Kielt, J.F., Kim, S.Y., Ladouceur, S., Ledu, D., Chen, L., Limoges, A., Londeix, L., Lu, S.H., Mahmoud, M.S., Marino, G., Matsouka, K., Matthiessen, J., Mildenhal, D.C., Mudie, P., Neil, H.L., Pospelova, V., Qi, Y., Radi, T., Richerol, T., Rochon, A., Sangiorgi, F., Solignac, S., Turon, J.L., Verleye, T., Wang, Y., Wang, Z. & Young, M.: Atlas of modern dinoflagellate cyst distribution based on 2405 data points, *Review of Palaeobotany and Palynology*, 191, pp. 1-197, DOI: 10.1016/j.revpalbo.2012.08.003, 2013.